ELSEVIER

Marine Geology 144 (1997) 81–96

MARINE GEOLOGY
INTERNATIONAL JOURNAL OF MARINE GEOLOGY, GEOCHEMISTRY AND GEOPHYSICS

Subaqueous delta of the Ganges–Brahmaputra river system

Steven A. Kuehl [a,*], Beth M. Levy [a], Willard S. Moore [b], Mead A. Allison [c]

[a] *Virginia Institute of Marine Science, College of William and Mary, Gloucester Point, VA 23062, USA*
[b] *Department of Geological Sciences, University of South Carolina, Columbia, SC 29208, USA*
[c] *Department of Oceanography, Texas A&M University, 5007 Avenue U, Galveston, TX 77551, USA*

Received 19 July 1996; accepted 16 June 1997

Abstract

The Ganges–Brahmaputra is among the world's three largest river systems in terms of sediment load, but, until now, no high-resolution seismic data have been obtained to document the nature of the sediment deposit seaward of the rivers' mouths. The other two (Amazon, Huanghe) discharge into energetic coastal environments and form subaqueous deltas with characteristic clinoform stratigraphy. High-resolution seismic reflection profiles of the Bengal shelf reveal similar stratigraphy: topset beds dip gently (0.036°) and diverge offshore; more steeply dipping foreset beds (0.190°) converge farther seaward; and relatively thin, gently dipping bottomset beds (0.022°) extend across the outer shelf, overlying an erosional surface presumed to be of Late Pleistocene age. Sediment accumulation rates are highest in the foreset region (≥5 cm/year) and reduced in the bottomset region (<0.3 cm/year), corroborating the relative thickening and thinning of strata observed in seismic profiles. Taken together, these data indicate a subaqueous delta is actively prograding across the Bengal shelf. Volume estimates for the Holocene subaqueous delta reveal that about one third of the total load of the Ganges–Brahmaputra has accumulated on the shelf. The remainder is likely partitioned between the river floodplain/delta plain and off-shelf transport via the submarine canyon, Swatch of No Ground. The canyon incises the shelf in the area of highest sedimentation rates (foreset), and growth faults and slumping of modern sediments near the head of the canyon support the idea that significant off-shelf transport of sediments to the Bengal Fan is occurring. © 1997 Elsevier Science B.V.

Keywords: delta; shelf sedimentation; seismic reflection profiling; sediment budget; Bay of Bengal; Ganges River; Brahmaputra River

1. Introduction

Modern river deltas have a range of characteristic morphologies that, to a first approximation, are controlled by the fluvial, tidal, and wave regime (Wright and Coleman, 1973). Deltas with extensive subaerial expression, such as the Mississippi delta, commonly are found in quiescent seas or protected locations such as fjords and embayments. Rivers entering energetic marine environments display a variety of morphologies. For example, the Columbia River (Northwest coast, U.S.A.) has no subaerial delta, rather, accumulation occurs as a mid-shelf mud deposit (Wright and Nittrouer, 1995). Rivers with sediment loads comparable to the Ganges–Brahmaputra, such as the Amazon and Huanghe, exhibit predominant

* Corresponding author. Fax: +1 (804) 684 7250;
e-mail: kuehl@vims.edu

PII S0025-3227(97)00075-3

or partial subaqueous growth of their deltas, respectively (Nittrouer et al., 1986; Prior et al., 1986; Alexander et al., 1991). Even though the sediment discharge of the Amazon is sufficient to produce a sizable subaqueous delta (clinoform) on the shelf, large shear stresses, generated primarily by tides, appear to prevent or limit significant subaerial growth in the vicinity of the river's mouth (Kuehl et al., 1986; Geyer et al., 1996). For the Huanghe, about 10–15% of the sediment discharge accumulates south of the Shangdong Peninsula as a subaqueous delta (Alexander et al., 1991), with much of the remaining discharge contributing to rapid subaerial growth. This dual-mode progradation of the delta reflects the phasing of river discharge and energy conditions in the Gulf of Bohai; high discharge occurs during low-energy conditions resulting in deposition near the mouth and significant subaerial growth (Wright and Nittrouer, 1995).

Although the combined sediment discharge of the Ganges–Brahmaputra river system is among the world's largest and its delta plain among the world's most densely populated, little is known regarding the Holocene evolution of the delta or the processes and patterns of recent deltaic sedimentation. Based on examination of nautical charts dating back some 200 years, Coleman (1969) suggested that no significant seaward progradation of the shoreline had occurred and that sediments discharged to the coastal ocean therefore escaped to the deep sea through the Swatch of No Ground, a major submarine canyon feeding the immense Bengal Fan. A recent critical examination of a more extensive set of historical charts, however, has provided evidence for some recent growth of the subaerial delta, but with progradation occurring in a lateral (west to east) fashion (Allison, 1997). Preliminary study of the continental shelf seaward of the rivers' mouths revealed significant sediment accumulation, leading to the suggestion that the observed clinoform-like morphology reflects the presence of an active subaqueous delta (Kuehl et al., 1989). However, until now, no seismic data have been obtained to document the stratigraphic nature of this feature. Here we report the results of the first high-resolution seismic reflection study conducted on the Bengal shelf seaward of the Ganges–Brahmaputra river system. In addition, sediment cores collected from the shelf are used to examine the distribution of recent accumulation rates in relation to seismic observations. The objectives are to examine the idea that a major component of the Ganges–Brahmaputra delta occurs on the shelf as a subaqueous clinoform and to evaluate the role of the Swatch of No Ground as a potential conduit for bypassing modern river sediments to the Bengal Fan.

2. Background

2.1. River characteristics and Holocene stratigraphy of the delta

The Ganges, Brahmaputra and Meghna rivers have occupied and abandoned numerous courses during the Quaternary and have deposited a large, flat, low-lying alluvial/delta plain encompassing most of the country of Bangladesh (Coleman, 1969). The Ganges drains the south slopes of the Himalayan mountains whereas the Brahmaputra mostly drains the north slopes, with estimated suspended sediment loads of 520×10^6 t/year and 540×10^6 t/year, respectively (Milliman and Syvitski, 1992). The Meghna River drains northeastern Bangladesh but has a negligible impact on the combined load of the system, contributing only about 1% of the total sediment discharge (Coleman, 1969). Combined monthly sediment and water discharge reaches a maximum in August during the southwest monsoon, with minimal levels (an order of magnitude less than peak rates) in January–March. Suspended sediments of the Ganges–Brahmaputra are coarse relative to other large river systems; at the confluence of the Ganges and Brahmaputra about 40% is sand (mostly fine–very fine) and 60% silt–clay (Barua et al., 1998).

Umitsu (1985, 1987, 1993) divided the landforms of the Bengal Basin into two geomorphological units: Pleistocene terrace uplands and recent alluvial lowlands (Fig. 1). The Pleistocene terraces are found in the marginal and interior portions of the Basin. In the north the uplands are known as the Barind Tract, and as the Madhupur Terrace

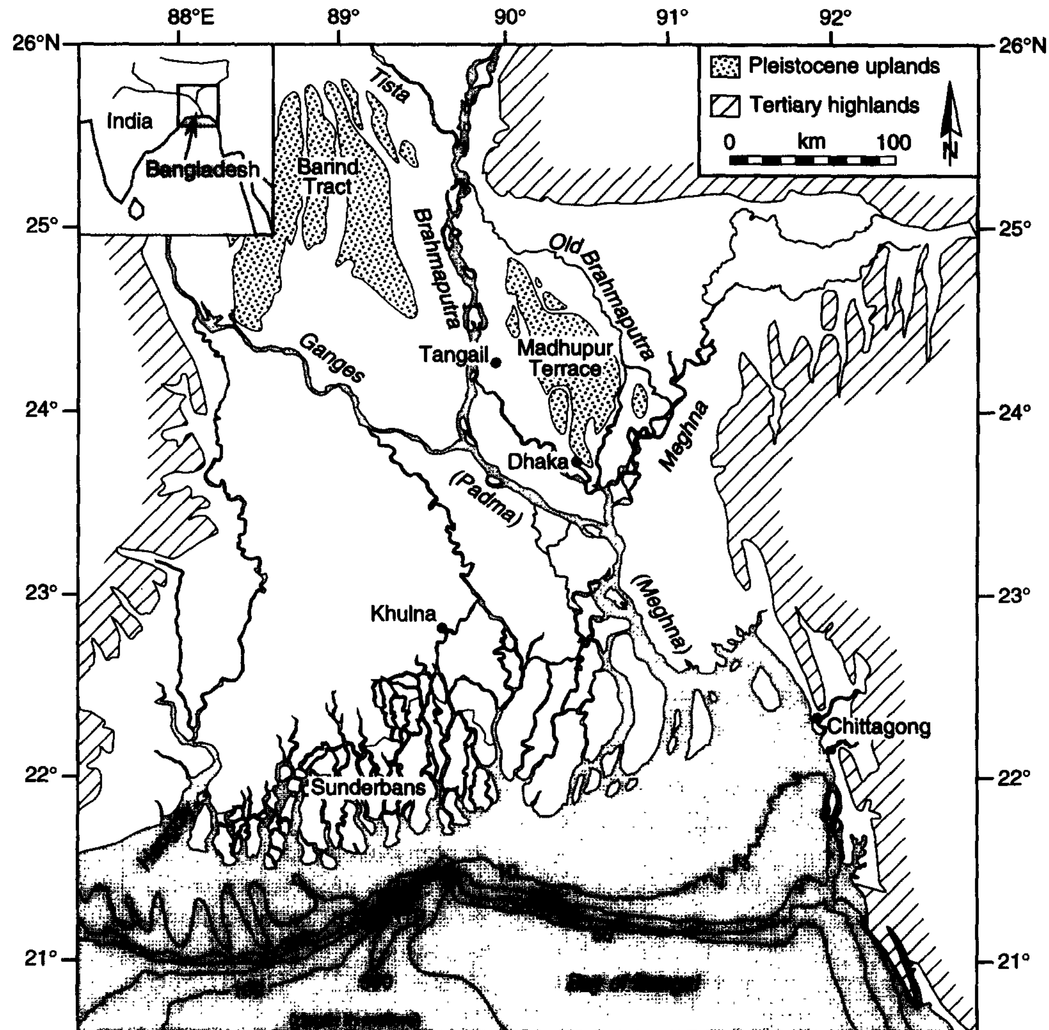

Fig. 1. Physiographic map of the Ganges–Brahmaputra delta.

in the central region. Alluvial lowlands are distributed widely over the Bengal Basin with characteristic levees, point bars and channel bars, as well as lower landform units such as swamps, marshes and former river channels. Sediments consist mainly of sand, silt, and clay layers with peat layers recognized in several places. The elevation of the lowlands typically is <15 m above sea level and most of the southern region is <3 m above sea level.

Five stratigraphic units characterize the evolution of the Ganges–Brahmaputra delta since the last glacial maximum (Umitsu, 1993). The *lowest unit* dates from the last glacial maximum and consists of sandy gravels deposited by the rivers down cutting older surfaces. Radiocarbon dating and similarities in sediment facies and grain size of the *lower* unit near Khulna City with that of the present Brahmaputra River flood plain suggest that this unit represents the flood plain about 12,000 years before present. The *middle unit* is composed of fine deltaic sediments deposited during the transgression. Peat layers are found in the Sylhet Basin in the lower horizon of the unit, indicating the presence of marshes during this period. The lower portion of the *upper unit* (mid-Holocene) is comprised of silt and clay in the inland region of Tangail; however, near the more coastal region of Khulna, the sediments exhibit a strong marine influence. Umitsu (1993) proposed that the coastline at that time retreated slightly north of the present Khulna City. The upper portions of the *upper unit* become coarser, with peat in places, suggesting that the coastline prograded during this time as broad marshy peat lands covered the central Ganges–Brahmaputra delta. During the late Holocene the rate of sea-level rise decreased, allowing fine silts and clays with intermittent peat layers to be deposited, here called the *uppermost unit*.

2.2. *Oceanography of the Bay of Bengal*

The Ganges–Brahmaputra river system discharges into an energetic marine environment characterized by strong tidal currents, moderate wave activity, seasonal monsoons and frequent cyclones. The mixing and subsequent spreading of the fresh water greatly affects the oceanography of the coastal waters. In addition to perennial discharge from the Ganges and Brahmaputra, seasonal discharges are introduced into the Western Bay from India via the Godavari, Krishna and Cauvery rivers (Suryanarayana et al., 1992). The advection and mixing of these fresh waters (about 2300 km^3/year) with the coastal ocean is controlled by external and internal forcing from wind and thermohaline conditions (Suryanarayana et al., 1992).

Seasonal low-pressure areas over the Persian Gulf during the summer and high pressure over the Tibetan Plateau during the winter create monsoonal winds, from the southwest in summer and from the northeast in winter (Murty et al., 1992). Changing monsoonal winds affect surface water flow in the open Bay of Bengal (Wyrtki, 1973). The spring is characterized by clockwise rotation, with the fastest flow close to the central Indian continental shelf, where it can reach 1.5–2.5 m/s. The autumn is characterized by counterclockwise movement with lower speeds in the eastern and central regions of the bay as opposed to the western region. Spring winds, combined with the Coriolis effect, result in the movement of surface water away from the east Indian coast with deeper water upwelling, causing the isopycnals to tilt upward towards the Indian coast. In the autumn, the reverse occurs as water is piled up in the western part of the bay and the isopycnals tilt down toward the east Indian coast. Resulting seasonal changes in sea level exceed 1 m for the northeast coast at Chittagong and along southeast Bangladesh, the largest on record (Murty et al., 1992). Observations and modeling of the fresh water emanating from the Ganges–Brahmaputra rivers' mouths indicate that during the period of maximum sediment and water discharge (June–September), the plume trajectory is along the coast toward the west (Shetye et al., 1996).

Tides in the coastal waters off Bangladesh primarily are semi-diurnal. The combined effects of Coriolis acceleration and the funnel shape of the bay produce an area of increased tidal amplitude along the eastern coast, typically about 4 m, decreasing to less than 2 m for the western portion of Bangladesh. For a small area between Hatia and Sandwip channels amplitudes of up to 6 m (Barua et al., 1994) and velocities exceeding 300 cm/s (Coleman, 1969) are observed.

Cyclones are common in the Bay of Bengal, and about 16% of cyclonic storms developing in the bay strike the Bangladesh coast (Mooley and Mohile, 1983). The frequency distribution of cyclone activity is distinctly bi-modal with peak activities in May and October, corresponding to the transition periods between the northeast and southwest monsoons.

2.3. *Sediment dispersal on the Bengal shelf*

Few published studies have addressed recent sediment dispersal on the Bengal shelf. Barua et al. (1994) show that the magnitude and distribution of suspended sediments during the low-discharge period are primarily a function of tidal energy in the nearshore region (< 15 m water depth). Sediments which are ≤ 125 μm (fine sand to clay) are continuously transported in suspension, except for brief periods during slack water. Based on mineralogical investigation of surficial sediments, Segall and Kuehl (1992) suggest that only during high-discharge periods (May–October) are significant amounts of sediment transported seaward of the 20-m isobath. Seabed textural and geochronological data reveal a westward fining along the mid-shelf area with a corresponding increase in sediment accumulation rates, suggesting westward transport along the shelf toward the Swatch of No Ground (Kuehl et al., 1989).

3. Methods

3.1. Field methods and seismic interpretation

A total of 450 km of GeoPulse® multifrequency seismic reflection data were obtained during a 1991 survey of the Bengal shelf along eight transects (Fig. 2), with maximum seabed penetration in excess of 100 m and vertical resolution of ~0.5 m. Seabed sampling retrieved nine kasten cores (3-m maximum length) and eleven grab samples. Sediment cores were subsampled by taking centimeter-thick sections, typically at 5- or 10-cm intervals, which were homogenized and bagged for sedimentological and geochemical analyses. A wood fragment recovered from the kasten-core nosepiece at Station 1 (~1.4 m depth in seabed) was saved for radiocarbon dating.

Navigation data from the 1991 cruise was converted from local Decca coordinates to latitude and longitude. Using a 3-point moving average, horizontal distances (in km) were determined along transects between each time mark, typically every 15 min. Vertical scales were calculated based on the recorder setting, assuming a velocity of 1500 m/s. The seismic profiles were collected in analog format using an EPC® graphic recorder, and key sections were digitally scanned at 400 dpi resolution. Scanned sections were cleaned, scaled, and mosaicked using Intergraph Microstation® and IRASB® vector/raster processing software.

3.2. Laboratory methods

Analyses of short-lived radioisotopes were performed using gamma spectroscopy. ^{210}Pb and ^{137}Cs activities were determined by direct measure-

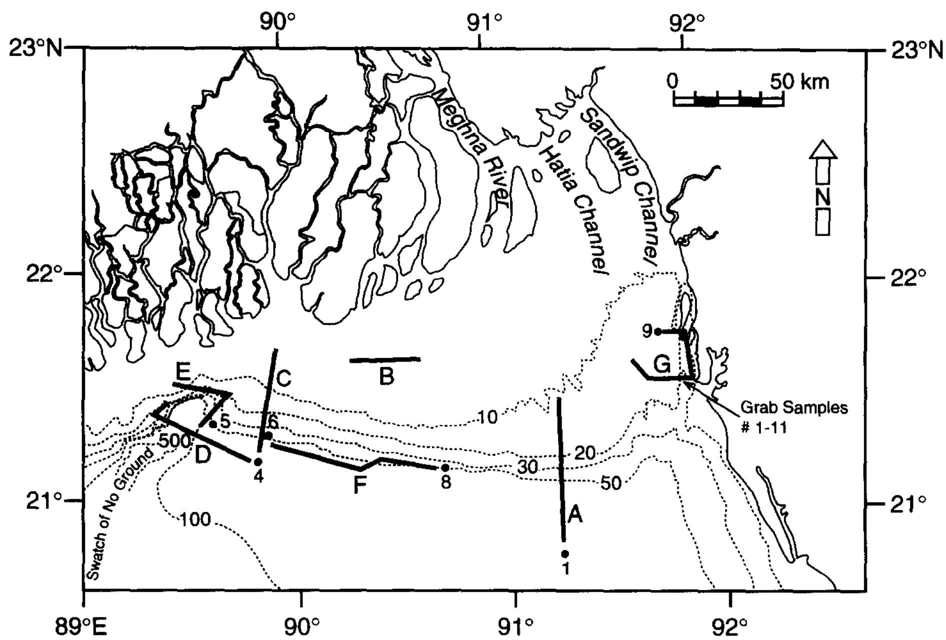

Fig. 2. Bathymetric chart of the Bengal shelf showing coring station locations (numbers) and seismic transects (letters). A major submarine canyon, 'Swatch of No Ground', incises the shelf along the western side of the study area.

ment of their characteristic gamma-ray emissions, whereas ^{226}Ra activities were determined indirectly through measurement of its short-lived daughters. Samples were packed in petri dishes (6.5 cm diameter by 2.25 cm), sealed to prevent loss of ^{222}Rn (an intermediate daughter between ^{226}Ra and its measured daughters, ^{214}Pb and ^{214}Bi) and to allow for ingrowth before counting. Self absorption corrections for ^{210}Pb were made using the methods of Cutshall et al. (1983).

Radiocarbon analysis was performed on the wood sample using the benzene synthesis and liquid scintillation counting method similar to that described by Polach and Stipp (1967).

Textural analyses were performed by wet sieving samples through a 63 μm sieve to separate the sand and mud (clay and silt) fractions. Sand was sieved at 1/2 ϕ intervals, and detailed analysis of the mud fraction was performed using a Sedigraph® model 5100 ET X-ray digital settling analyzer. Results of Sedigraph® and sieve analyses were combined to calculate grain-size and sorting statistics.

4. Results

4.1. Seismic profiles

The GeoPulse® records reveal clinoform stratigraphy for the sediment wedge off the Ganges–Brahmaputra rivers' mouths (Fig. 3). The clinoform thickness exceeds 60 m on the middle shelf, thinning to <10 m at the seaward limit of the profiling. Five regions of the shelf have been delineated based on regional variations in acoustic character of the seabed and are described below.

4.1.1. Nearshore (5–15 m)

Seismic profiles from the nearshore region of the Bengal shelf reveal a highly reflective sediment surface with limited acoustic penetration (<25 m) and few distinct subsurface reflectors (Fig. 4), characteristic of high sand content. In the northeastern section of the bay, along the Chittagong coast, asymmetrical sand waves ranging in height from 3 to 5 m (Fig. 5) are present in the channel (Fig. 2) which presumably is related to the struc-

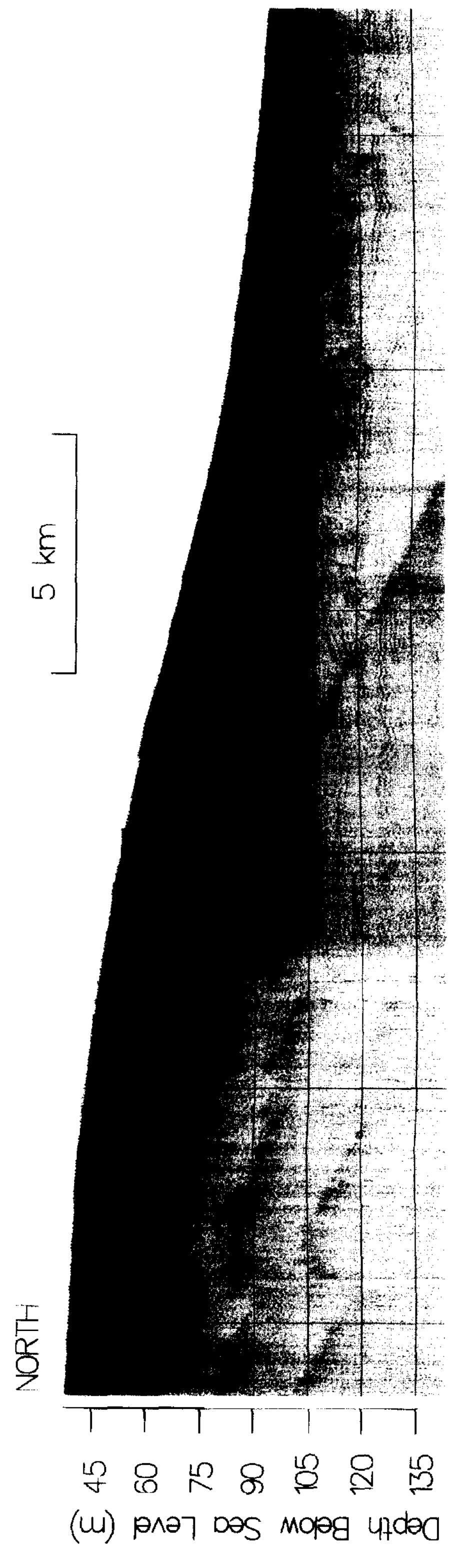

Fig. 3. GeoPulse® record from transect *A* showing clinoform stratigraphy for the Holocene sediment wedge on the Bengal shelf. The modern subaqueous delta is prograding over Pleistocene strata which are seen as irregular reflectors underneath bottomset beds of the clinoform below about 100 m. Subsurface foreset beds between about 60 to 75 m (northern portion of profile) display zones of acoustically transparent sediment which may result from mass movement (cf. Fig. 7).

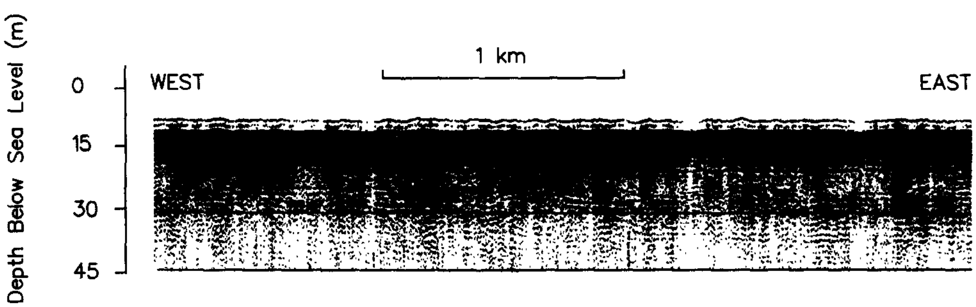

Fig. 4. GeoPulse® record from the near-shore (transect *B*) revealing poor acoustic penetration, probably a result of the high abundance of sand in this region. The thin (2–3 m) surface unit may represent a veneer of mud (probably ephemeral) overlying sand typical of the inner topset region.

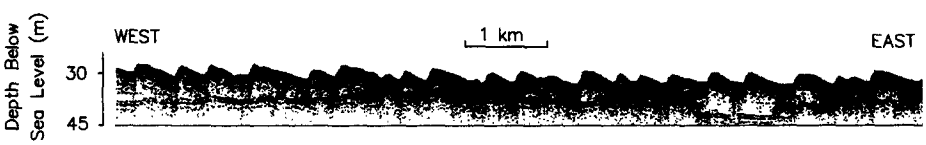

Fig. 5. GeoPulse® record from the eastern region of the study area (transect *G*) showing asymmetrical sand waves indicating transport toward the west. Grab samples from this area reveal clean medium sand.

tural troughs of the adjacent Chittagong hill tracts. The sand waves appear to be more widely spaced toward the west, in the direction of the lee face. Very shallow (<15 m) acoustic penetration was achieved in this area and field descriptions of surficial grab samples indicate a well-sorted medium sand.

4.1.2. *Inner shelf (15–30 m)*

Closely spaced acoustic reflectors (<2–3 m spacing) are present in the shallow seabed (upper 15 m) for much of the inner-shelf region. These reflectors are underlain by an irregular erosional surface in transects A and C that has an areal extent of at least 720 km². The erosional surface displays cut and fill features perhaps associated with subaqueous distributary channels (Fig. 6).

The inner shelf dips gradually seaward in this region, with an average gradient of 0.036°. No significant change in this gradient is observed from east to west. Farther seaward, in water depths of ~30 m, greater than 30 m of subbottom penetration is achieved and previously-parallel reflectors begin to diverge (Fig. 3). The spacing between reflectors increases from <2–3 to ~5 m with distance from shore.

4.1.3. *Middle shelf (30–60 m)*

Densely spaced reflectors (3–5 m spacing) are observed in the middle-shelf region where typical acoustic penetration between 30 and 45 m is achieved. The beds begin to converge seaward in water depths of about 60 m (Fig. 3), where reflector spacing is reduced to <2–3 m. Individual beds

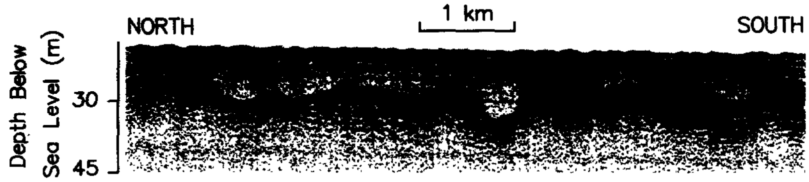

Fig. 6. GeoPulse® record from the inner shelf (transect *C*) revealing an erosional surface beneath thin topset beds. The cut and fill features could reflect migration of subaqueous distributary channels.

are difficult to discern in the seaward portion of the middle shelf and irregular, erosional surfaces can be seen below the stratified sediments. The gradient of the sediment wedge over the middle shelf averages 0.19°. This gradient appears to be uniform from the eastern transect to the Swatch of No Ground.

Two distinct acoustically transparent layers, about 3–5 m thick, are observed both from shore perpendicular and shore parallel transects. Located at depths of ~10 and ~20 m below the sediment surface, the layers are roughly parallel to one another and to the seabed surface (Fig. 7). The acoustically transparent layers pinch out in water depths of about 80 m on the outer shelf. Based on the seismic data, the layers appear to have an areal extent of ~1500 km^2, extending at least 12 km north–south and 127 km east–west.

4.1.4. Outer shelf (60–>80 m)

Profiles from the outer-shelf region reveal closely spaced (<2–3 m spacing), parallel acoustic reflectors extending to water depths of at least 80 m, the seaward extent of the seismic lines. The seafloor gradient in this area is very gentle, 0.022°. An erosional contact is seen below the shallow strata relatively close to the seabed surface (within ~10 m). The erosional contact is uneven and displays varying relief, with distinct cut-and-fill features (Fig. 8). Strata underlying this reflector are discontinuous with indistinct bedding.

4.1.5. Swatch of No Ground

Profiles near the Swatch of No Ground (Figs. 9 and 10) reveal increased acoustic penetration relative to the eastern and nearshore shelf regions of similar water depths. On the western side of the canyon, a well-stratified seabed is observed, containing distinct, parallel, and continuous acoustic reflectors with typical spacing of 3–5 m between beds. On the eastern side of the canyon, beds are also densely spaced but are more irregular in nature than their western counterparts.

Abundant growth faults and slumps are found on the eastern flanks of the canyon. Slumps with rotational movement to the west are observed along the margin of the canyon (Fig. 9). An east–west trending gully feeds into the canyon with growth faults along the south side dipping steeply into the canyon (Fig. 10). Near the canyon head, strata become more irregular and often are chaotic, with discontinuous and truncated beds. Profiles of the canyon floor near its head show irregular strata with few discernible beds and an uneven sediment surface.

4.2. Sediment accumulation rates

Sediment accumulation rates were estimated primarily using ^{137}Cs and, in one instance, corroborated by ^{210}Pb geochronology. In most cases, ^{210}Pb profiles could not be modeled as steady-state accumulation because activities fluctuate markedly down core, in part a result of grain-size variations (Kuehl et al., 1989). In these cases, the penetration depths of ^{137}Cs were used to provide a first-order estimate (Table 1). As ^{137}Cs has been present worldwide in measurable quantities since about 1954, the depth to which ^{137}Cs is observed in the cores divided by the number of years since introduction (in this case 37 years) provides a rough estimate of the sediment accumulation rate. A

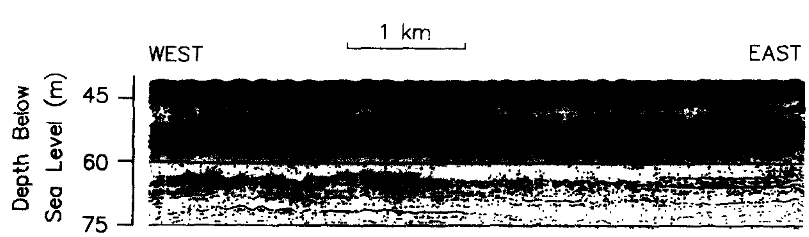

Fig. 7. GeoPulse® record from the foreset beds (transect F) showing two distinct acoustically transparent beds at about 48 m and 62 m. The ~5-m thick transparent beds extend at least 100 km along the foreset region and probably represent large-scale mass movement, perhaps triggered by cyclones or earthquake activity common to the area.

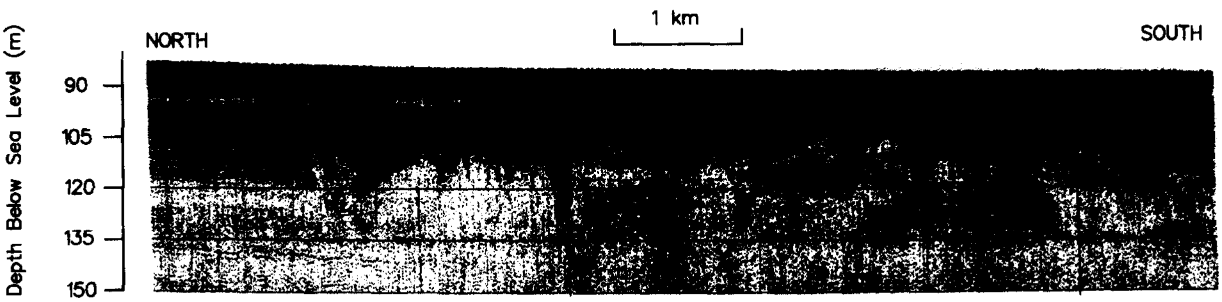

Fig. 8. GeoPulse® record from the seaward portion of transect C, showing thin parallel bottomset beds overlying Pleistocene strata below about 100 m. Cut and fill features are evident in the Pleistocene strata suggesting former channels or gullies.

potential problem with this approach is the effect of seabed mixing (physical or biological) on ^{137}Cs profiles, which would increase penetration depths and lead to an overestimate of sediment accumulation rate. Areas most susceptible to this effect would be those experiencing low accumulation rate ($< \sim 1$ cm/year) and/or deep intense mixing. Previous studies have shown that physical sedimentary structures dominate the inner and middle shelf area (Segall and Kuehl, 1994), indicating that biological mixing is unlikely to affect ^{137}Cs penetration depths in these areas. Deep physical mixing, such as that observed for the Amazon delta (Kuehl et al., 1995), would most likely be a problem in shallow water depths ($< \sim 20$ m) where the effects of waves and tides are most pronounced. Most of the cores examined for this study were collected in water depths > 20 m (Fig. 2). Using ^{137}Cs penetration depth as a first-order estimate, a sediment accumulation rate of 1.8 cm/year is obtained for a core collected in a shallow trough in the eastern part of the inner shelf (Station 9). This rate could represent a minimum because ^{137}Cs is present throughout the core, thus the actual first appearance of ^{137}Cs in the seabed may be deeper. Kasten cores could not be obtained from the nearshore region because of the presence of sands, which hinders gravity coring. For the middle-shelf area, sediment accumulation rates were 1.1 cm/year (Station 6) and 0.6 cm/year (Station 4). The highest sedimentation rates are found in the area surrounding the Swatch of No Ground. Station 5 revealed a minimum rate of 5.2 cm/year, based on the presence of ^{137}Cs throughout the core. For the outer shelf Station 1, sediment accumulation rates were derived using both ^{137}Cs and ^{210}Pb profiles, with a maximum rate of 0.3 cm/year. Although some evidence of bioturbation was noted at this station (indicating the reported rate may be a maximum), the accumulation rate was the lowest measured in this study. Radiocarbon dating of a wood fragment collected from the nosepiece at Station 1 gave an age of $10,000 \pm 240$ year.

4.3. *Grain-size analysis*

Textural analyses were performed on samples from six cores (Table 2). Cores from the western middle shelf (Stations 4, 5 and 6) are very fine-grained, with down-core average means of 8.5 ϕ for Stations 4 and 5, as compared with an average mean of 7.0 ϕ for Station 8 on the central middle shelf. The cores from the outer shelf (Station 1) and from the shallow trough in the eastern inner shelf (Station 9) have intermediate average means of 7.9 ϕ and 7.6 ϕ, respectively.

5. Discussion

5.1. *Subaqueous delta*

A distinctive morphology can be seen in the sediment wedge prograding southward and westward from the rivers' mouths on the inner Bengal shelf (Fig. 11). The seismic profiles reveal the gently sloping topset, more steeply dipping foreset, and gently sloping bottomset stratigraphy characteristic of subaqueous deltas (Fig. 3). On the inner

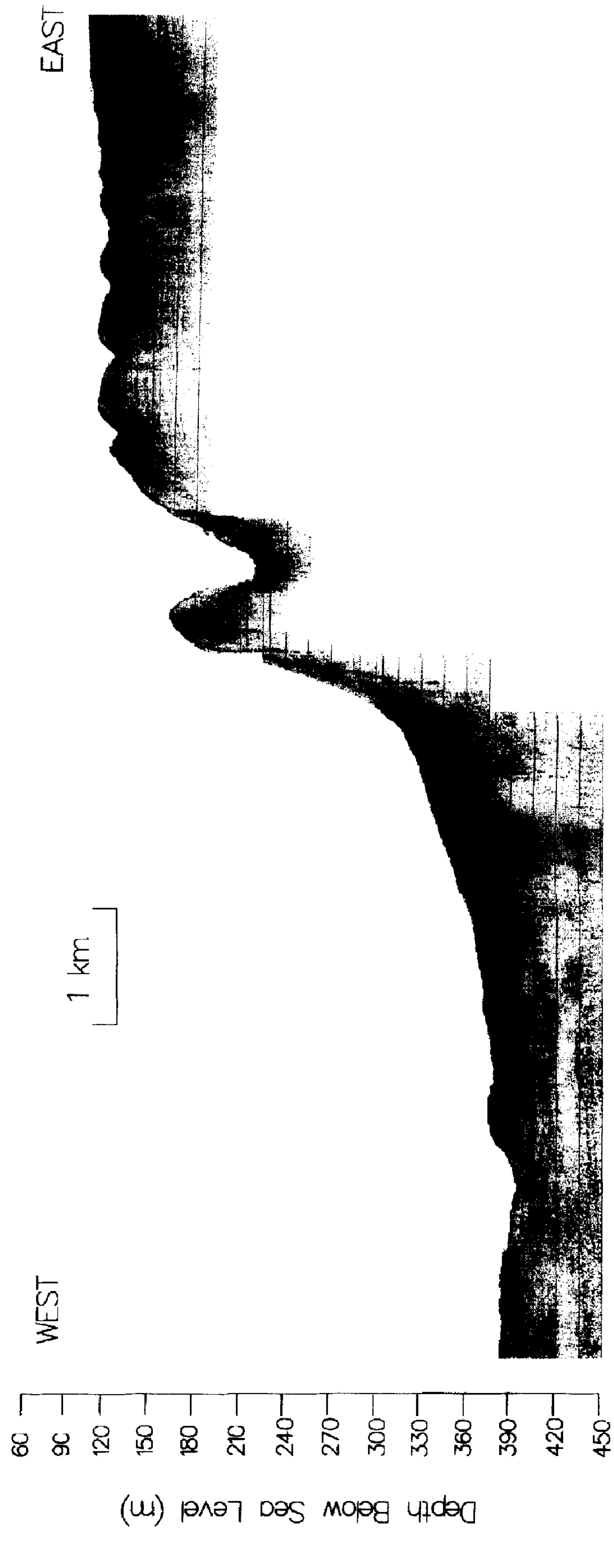

Fig. 9. GeoPulse® record from the head of the submarine canyon, Swatch of No Ground (east–west leg of transect *E*). A series of four large (~0.5 km) slump blocks are seen at the edge of the shelf. Reflectors within the slump blocks dip east, back towards the shelf. Below the shelf edge the profile crosses a deep (~60 m) gully before falling off to the canyon floor. A hummocky sediment surface on the canyon floor suggests mass movement of sediment from the shelf into the canyon.

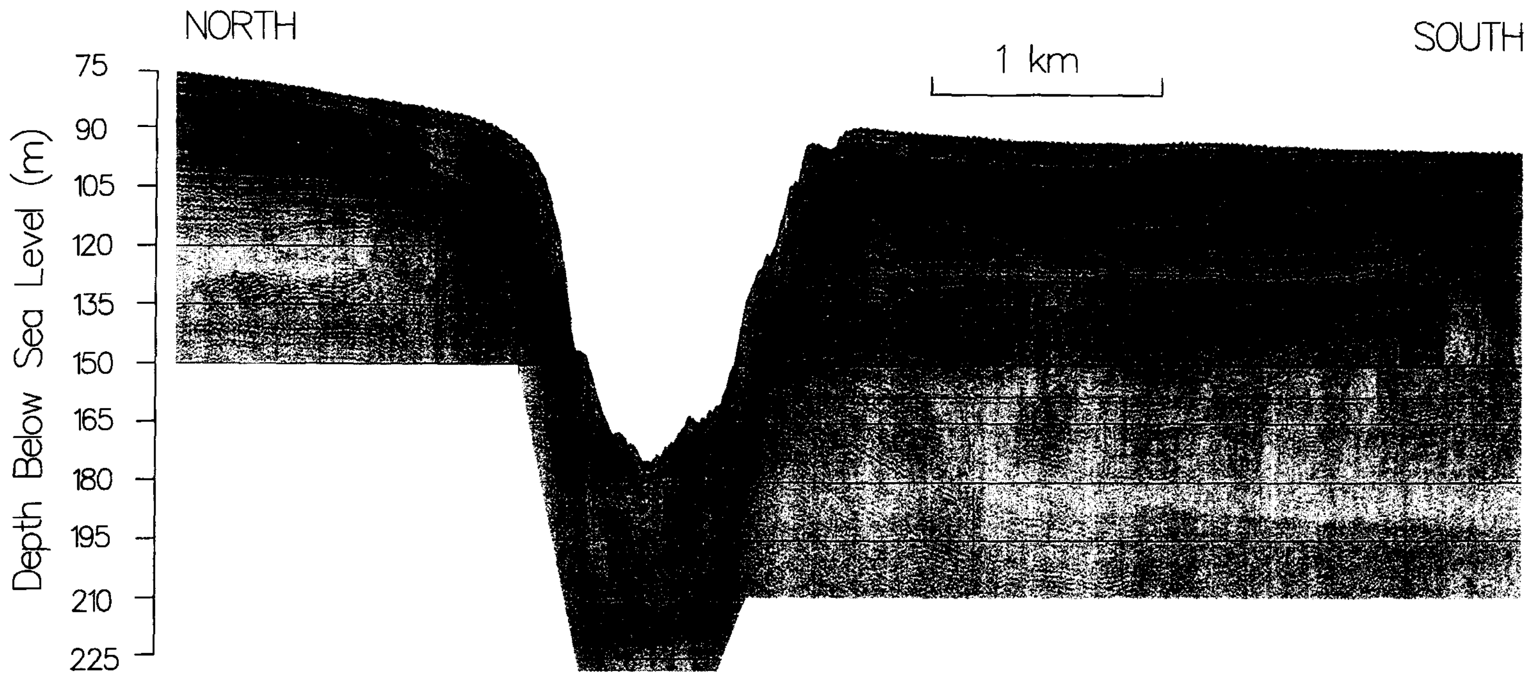

Fig. 10. GeoPulse® record across a gully on the eastern side of the Swatch of No Ground (northeast–southwest leg of transect *E*). A series of growth faults is present along the south edge with shear planes dipping down into the gully with decreasing angles towards the south. Deep subbottom acoustic penetration (> 100 m), along with the growth faults and deformed strata at depth, suggest rapid accumulation of fine-grained sediment. The hummocky sediment surface of the gully floor suggest mass movement into the gully/canyon system.

Table 1
^{137}Cs-based accumulation rates

Station Nr.	Core length (cm)	^{137}Cs penetration (cm)	Accumulation rate (cm/year)
1	81	11	0.3
4	151	21	0.6
5	191	191	>5.2
6	50	40	1.1
9	66	66	>1.8

shelf, in water depths of about 15–25 m, reflectors are nearly parallel and slope gently seaward. This trend gives way to divergent beds at the seaward edge of the topset region, evidenced by increased spacing between reflectors, indicating increased sedimentation rates. At depths of ~30 m the seafloor gradient increases abruptly (from 0.036° to 0.19°) and reflectors converge seaward across the foreset region. In the bottomset region (>60 m water depth) near-surface reflectors once again take on a semi-parallel appearance with strata that are closely spaced and thin. A hiatal surface is seen below the bottomset beds with evidence of uneven truncated beds and relict channels. A wood fragment from the core catcher at Station 1 was radiocarbon dated at ~10,000 years, suggesting that the underlying surface is most likely Pleistocene in age. Sediment accumulation rates obtained from this study indicate that the subaqueous delta is an active feature. High accumulation rates are observed for the thickest (foreset) part of the clinoform, ranging from about 1–>5 cm/year, and rates decrease to <0.3 cm/year in the bottomset region. Although accumulation rates were not determined for the nearshore topset region, the abundance of coarse (sandy) sediment indicates bypassing of fine-grained sediment to the middle and outer-shelf areas.

5.2. Shelf sediment dispersal

Textural and acoustical characteristics of the seabed provide clues to patterns of shelf sediment dispersal. In the nearshore region, poor acoustic penetration (0–25 m) and our inability to collect long gravity cores suggest a sandy seabed. Along the eastern margin, near Chittagong, sand waves are observed and field descriptions of grab samples from this area reveal a clean medium sand. The sand waves have considerable relief (3–5 m), implying a high-energy environment. The orienta-

Table 2
Grain-size data

Sample	Mean depth (cm)	Mean grain size (ϕ)	Average mean for core	Sorting
Core 1				
A911-0	1.0	6.9	7.9	3.5
A911-20	21.0	8.1		2.4
A911-30	31.0	6.5		4.0
A911-80	81.0	7.6		2.4
A911-100	101.0	8.7		2.6
A911-140	141.0	9.5		2.6
Core 4				
A914-8	9.0	6.9	8.5	2.1
A914-15	16.0	9.8		1.8
A914-25	26.0	8.4		2.5
A914-55	56.0	8.2		2.2
A914-65	66.0	8.4		2.1
A914-90	91.0	8.3		2.5
A914-140	141.0	9.1		2.3
A914-160	161.0	8.8		2.4
A914-200	210.0	8.2		2.7
Core 5				
A915-0	1.0	8.7	8.5	2.0
A915-20	21.0	9.4		2.2
A915-25	26.0	7.4		2.4
A915-40	41.0	8.1		2.3
A915-75	76.0	8.7		2.1
A915-100	101.0	9.0		2.1
A915-130	131.0	8.0		1.7
A915-140	141.0	8.7		2.2
Core 6				
A916-0	1.0	7.9	7.9	2.4
Core 8				
A918-0	1.0	7.0	7.0	1.9
A918-8	9.0	7.0		2.4
A918-15	16.0	6.9		2.3
A918-25	26.0	6.9		2.3
Core 9				
A919-0	1.0	8.6	7.6	3.3
A919-2	3.0	7.4		2.1
A919-10	11.0	9.0		0.7
A919-15	16.0	8.4		1.2
A919-45	46.0	5.6		2.6
A919-50	51.0	6.7		2.7

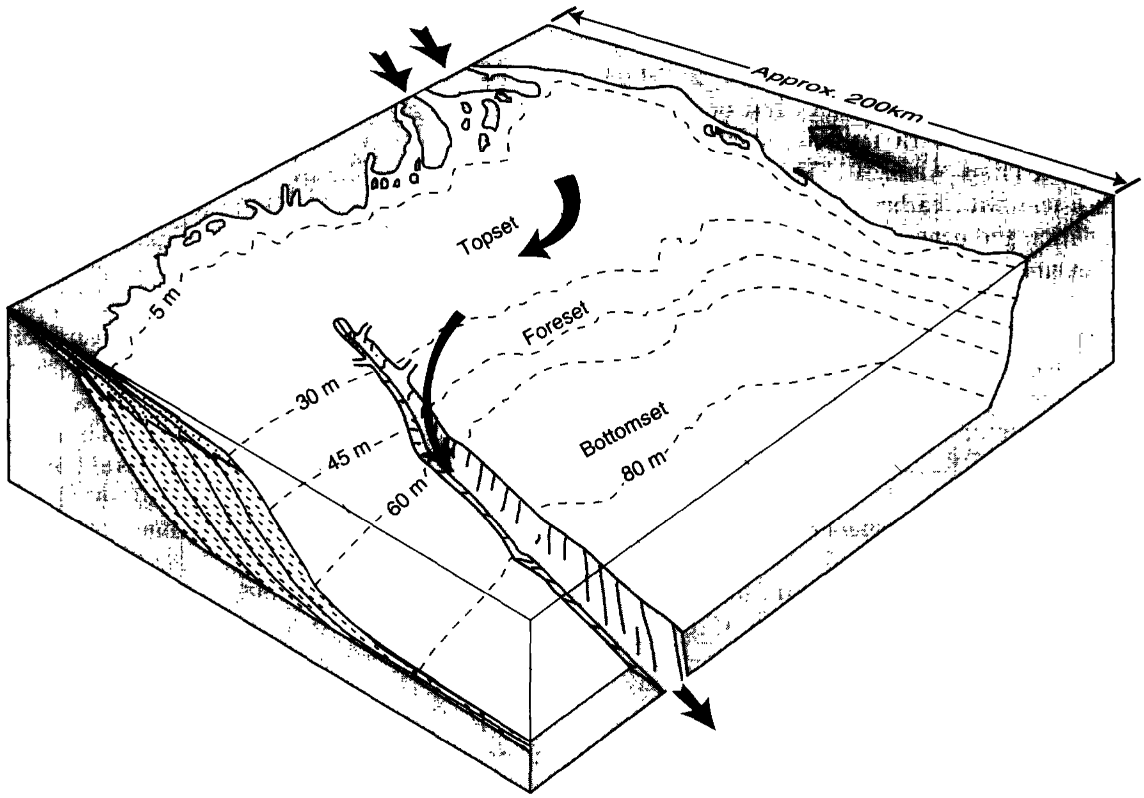

Fig. 11. Cartoon illustrating features of the subaqueous delta on the Bengal shelf seaward of the Ganges–Brahmaputra river system. The clinoform is characterized by relatively coarse-grained (sand) topset beds and fine-grained (mud) foreset and bottomset beds. Evidence from a variety of sources indicates that a significant fraction of sediment discharged to the shelf is transported seaward and westward along the shelf, and escapes to the deep sea through the Swatch of No Ground.

tion of lee and stoss sides of the sand waves indicates east to west flow direction (Fig. 5). These features disappear toward the west, and acoustic penetration gradually increases as the sediment becomes finer. Along the middle shelf, textural analyses suggest a fining trend westward from Station 8 (7.0 ϕ) toward Station 6 (7.9 ϕ) and 5 (8.5 ϕ), near the Swatch of No Ground. Surface grain-size distributions from grab samples demonstrate a similar pattern of westward fining (Kuehl et al., 1989). The highest acoustic penetration is observed near the canyon (>100 m) indicating thick deposits of fine-grained sediments.

The evidence above indicates southward and westward transport of fine-grained sediments from the rivers' mouths toward the Swatch of No Ground. Energetic waves and currents at times of maximum sediment discharge likely prevent rapid accumulation of fine-grained sediments near shore. Westward sediment transport is evidenced by fining towards the west, sand wave orientation, and increased sedimentation rates near the Swatch of No Ground. This seabed evidence is corroborated by physical oceanographic observations and modeling which indicates westward extension of the river plume during the southwest monsoon (Shetye et al., 1996).

The Swatch of No Ground appears to divert the westward dispersal of sediments from the shelf into the canyon. This is supported by clay mineralogical studies which show a depletion of chlorite on the western side of the canyon, indicating that transport of chlorite-rich Brahmaputra sediment is interrupted by the canyon (Segall and Kuehl, 1992). The Swatch of No Ground incises the middle shelf in the western foreset region, the area of highest measured sedimentation rates (>5 cm/year). Evidence of mass movement is common in areas surrounding the canyon. High rates of sediment loading are one cause of sediment failures such as growth faulting, slumping, and mud flowage (Figs. 9 and 10). These observations are consistent with earlier studies showing rapid accumulation and penecontemporaneous deformation of sediment fabric in the vicinity of the canyon (Kuehl et al., 1989, 1991). The existence of growth faults and slumps directed into the canyon, coupled with the irregular, thick sequences of sediment found at the bottom of the canyon, is dramatic evidence that some sediment is bypassing the shelf via the Swatch of No Ground, presumably to the Bengal Fan.

Evidence of mass movement is also observed in the relatively steep foreset region of the subaqueous delta where two distinct, acoustically transparent layers are observed from the GeoPulse® profiles (Fig. 7). The transparent layers extend from the outer topset to inner bottomset beds, following the gradient of the subaqueous delta, and have an areal extent of ~1500 km^2. One possible explanation for these features is that they represent large-scale mud flows similar to those observed off the Mississippi River (Wright and Coleman, 1974). The widespread nature of these features suggests large-magnitude external forcing for failure. Such forcing could be accomplished by cyclones or earthquake activity common in the study area.

5.3. Volume of Holocene sediment wedge

In order to examine the significance of subaqueous deltaic progradation for the Ganges–Brahmaputra system since the maximum Holocene transgression, a first-order estimate was made of the volume of the sediment wedge forming on the inner shelf. Areal boundaries were delineated primarily based on seismic data from this study, stratigraphic analysis and interpretation of Umitsu (1993), and geographic information. Extrapolation of Umitsu's bore-hole data to the offshore enables estimates for the thickness of subaerial and subaqueous components of Holocene sediments deposited seaward of the maximum transgressive shoreline.

The Khulna region is considered the northernmost extent of the Ganges–Brahmaputra delta shoreline during the Holocene (Umitsu, 1993). Two fossil molluscs, *Corbiculidae geloina* and *Neritiolae neritina*, found at a depth of 16 m suggest that this was once a tidal environment. Radiocarbon dating of wood fragments found in the core at a depth of 16 m below sea level reveal an approximate age of 7000 ^{14}C years before present (Umitsu, 1993). The 7000-year shoreline is extrapolated laterally from Khulna for the volume estimates. In the east, the mountainous Chittagong hill tract provides a natural boundary. A southern boundary is provided by the 80-m isobath; bottomset beds are thin at this water depth and immediately overly the Pleistocene surface. The western boundary is taken to be the Hooghly River, just to the west of the Swatch of No Ground, which was a major outlet for the Ganges River in recorded history. Bathymetric and topographic data were used to constrain the upper surface, and the lower surface was taken as a plane extrapolated landward from the ~80-m isobath. All depth/elevation and position information was processed using Surfer® to calculate the volumes for the marine (1.97×10^{12} m^3) and terrestrial (0.26×10^{12} m^3) sediment accumulation seaward of the Holocene maximum transgression.

Based on the estimated annual sediment load of 1060×10^6 t/year (Milliman and Syvitski, 1992), the volume of marine material on the shelf (integrated over 7000 years and assuming a dry bulk density of 1.1 g cm^{-3}) represents about 31% of the rivers' input. The corresponding terrestrial portion is about 4.2%. Error of these budget estimates likely is large as they are based on modern sediment discharge figures that may not be representative of the entire late Holocene. For example, anthropogenic activities can have significant effects on sediment discharge; farming can increase load whereas river-control structures, such as dams, can reduce the load through trapping. Uncertainty in the chronology taken from Umitsu (1993) contributes further to the potential error of this estimate. Most importantly, the boundaries were based on sedimentary facies and geographical features and are, as such, arbitrary to some degree. Despite these uncertainties, the subaqueous delta off the Ganges–Brahmaputra clearly represents a significant component of the late Holocene delta.

In comparing the integrated discharge values to the volume of the subaqueous delta, an important consideration is that river discharge measurements are taken some distance upstream of the shoreline and may not reflect the amount supplied to the coastal ocean. Floodplain sedimentation appears to be a significant factor, accounting for a loss of 10–40% of the measured discharge for the Mississippi, Amazon and Changjiang rivers (Kesel et al., 1992; Nittrouer et al., 1995; Xiqing, 1996). For the Ganges–Brahmaputra system, estimates of floodplain sequestering range as high as 80% of the discharge, although these estimates are based on a limited data set (Milliman and Syvitski, 1992). Because floodplain accommodation could significantly reduce the rivers' input to the shelf, the proportion of sediment accumulation represented by the subaqueous delta could easily exceed the above estimate of 31%. A recent study of floodplain sedimentation rates for a 110 km reach of the Brahmaputra left bank estimates the removal of about 5% of the river's load (Allison et al., 1998); however, extrapolation of this figure to the rest of the floodplain and delta plain is problematic as considerable regional variation in floodplain sedimentation rates in this dynamic and tectonically complex region seems likely. More detailed study is needed to ascertain the role of the floodplain sedimentation in the overall budget.

6. Conclusions

(1) Seismic reflection profiles of the sediment wedge seaward of the Ganges–Brahmaputra river system reveal clinoform stratigraphy characteristic of a subaqueous delta. Sediment accumulation rates are highest in the foreset region (1–>5 cm/year) and decrease in the bottomset region (<0.3 cm/year), an observation consistent with an actively prograding clinoform.

(2) Seabed evidence suggests that the dominant transport of fine-grained sediment on the Bengal shelf is to the south and west. Sediments fine seaward and westward, with the thickest accumulation of mud near the submarine canyon, Swatch of No Ground, which incises the western shelf. Sand waves found near the eastern coast of Chittagong are oriented with their lee side facing west, also indicating westward transport.

(3) Slumps, growth faults and evidence of mass movement coupled with high sedimentation rates near the Swatch of No Ground provide dramatic evidence that modern sediment is being channeled off-shelf through the submarine canyon to the Bengal Fan.

(4) Sediment volume estimates reveal that the Holocene subaqueous delta accommodates about 30% of the rivers' load, indicating that subaqueous deltaic progradation is an important sink for the rivers' sediment. The remainder is partitioned between the floodplain/delta plain and deep sea, but the relative importance of these sinks is not known.

Acknowledgements

The authors would like to thank the Netherlands sponsored Land Reclamation Project for their logistical support during the field work. Financial support was provided by the National Science Foundation grants OCE-9019472 and OCE-9322254. Charles A. Nittrouer generously provided access to his GeoPulse® system used in the field study. Steven L. Goodbred drafted Fig. 1. This paper forms contribution No. 2069 from the Virginia Institute of Marine Science, College of William and Mary.

References

Alexander, C.R., DeMaster, D.J., Nittrouer, C.A., 1991. Sediment accumulation in a modern epicontinental-shelf setting: The Yellow Sea. Mar. Geol. 98, 51–72.

Allison, M.A., 1997. Historical changes in the Ganges–Brahmaputra delta front. J. Coastal Res., in press.

Allison, M.A., Kuehl, S.A., Martin, T., 1998. The importance of floodplain sedimentation for river sediment budgets and terrigenous input to the oceans: Insights from the Brahmaputra–Jamuna River. Geology, submitted.

Barua, D.K., Kuehl, S.A., Miller, R.L., Moore, W.S., 1994.

Suspended sediment distribution and residual transport in the coastal ocean off of the Ganges–Brahmaputra river mouth. Mar. Geol. 120, 41–61.
Barua, D.K., Martin, T.C., Hasan, A., Mahmood, S., Kuehl, S.A., 1998. Suspended sediment transport through the Ganges–Brahmaputra fluvial system: Implications for floodplain sedimentation and sediment delivery to the ocean. Sediment. Geol., submitted.
Coleman, J.M., 1969. Brahmaputra River: Channel processes and sedimentation. Sediment. Geol. 3, 129–239.
Cutshall, N.H., Larsen, I.L., Olsen, C.R., 1983. Direct analysis of ^{210}Pb in sediment samples: Self-absorption correction. Nucl. Instrum. Methods 206, 309–312.
Geyer, W.R., Beardsley, R.C., Lentz, S.J., Candela, J., Limeburner, R., Johns, W.E., Castro, B.M., Soares, I.D., 1996. Phys. Oceanogr. Amazon Shelf 16, 575–616.
Kesel, R.H., Yodis, E.G., McCraw, D.J., 1992. An approximation of the sediment budget of the lower Mississippi river prior to major human modification. Earth Surf. Process. Landf. 17, 711–722.
Kuehl, S.A., DeMaster, D.J., Nittrouer, C.A., 1986. Nature of sediment accumulation on the Amazon continental shelf. Cont. Shelf Res. 6, 209–225.
Kuehl, S.A., Hariu, T.M., Moore, W.S., 1989. Shelf sedimentation off the Ganges–Brahmaputra river system: Evidence for sediment bypassing to the Bengal fan. Geology 17, 1132–1135.
Kuehl, S.A., Hariu, T.M., Sanford, M.W., Nittrouer, C.A., DeMaster, D.J., 1991. Millimeter-scale sedimentary structure of fine-grained sediments: Examples from continental margin environments. In: Bennett, R.H., Bryant, W.R., Hulbert, M.H. (Eds.), Microstructure of Fine-Grained Sediments. Springer, New York, pp. 33–45.
Kuehl, S.A., Pacioni, T.D., Rine, J.M., 1995. Seabed dynamics of the inner Amazon shelf: temporal and spatial variability of surficial strata. Mar. Geol. 125, 283–302.
Milliman, J.D., Syvitski, J.P.M., 1992. Geomorphic/tectonic control of sediment discharge to the ocean: The importance of small mountainous rivers. J. Geol. 100, 525–544.
Mooley, D.A., Mohile, C.M., 1983. A study of cyclonic storms on the different sections of the coast around the Bay of Bengal. Mausam (India) 43, 139–152.
Murty, V.S.N., Sarma, Y.V.B., Rao, D.P., Murty, C.S., 1992. Water characteristics, mixing and circulation in the bay of Bengal during southwest monsoon. J. Mar. Res. 50, 207–228.
Nittrouer, C.A., Kuehl, S.A., DeMaster, D.J., Kowsmann, R.O., 1986. The deltaic nature of Amazon shelf sedimentation. Geol. Soc. Am. Bull. 97, 444–458.
Nittrouer, C.A., Kuehl, S.A., Sternberg, R.W., Figueiredo, A.G., Faria, L.E.C., 1995. An introduction to the geological significance of sediment transport and accumulation on the Amazon continental shelf. Mar. Geol. 125, 177–192.
Polach, H.A., Stipp, J.J., 1967. Improved synthesis technique for methane and benzene radiocarbon dating. Int. J. Appl. Radiat. Isot. 18, 359–364.
Prior, D.B., Yang, Z.S., Bornhold, B.D., Geller, G.H., Lin, Z.H., Wiseman Jr., W.J., Wright, L.D., Lin, T.C., 1986. The subaqueous delta of the modern Huanghe (Yellow River). Geo-Mar. Lett. 6, 67–75.
Segall, M.P., Kuehl, S.A., 1992. Sedimentary processes on the Bengal shelf as revealed by clay-size mineralogy. Cont. Shelf Res. 12, 517–541.
Segall, M.P., Kuehl, S.A., 1994. Sedimentary structures on the Bengal shelf: a multi-scale approach to sedimentary fabric interpretation. Sediment. Geol. 93, 165–180.
Shetye, S.R., Gouveia, A.D., Shankar, D., Shenoi, S.S.C., Vinayachandran, P.N., Sundar, D., Michael, G.S., Nampoothiri, G., 1996. Hydrography and circulation in the western Bay of Bengal during the northeast monsoon. J. Geophys. Res. 101, 14011–14026.
Suryanarayana, A., Murty, C.S., Rao, D.P., 1992. Characteristics of coastal waters of the western bay of Bengal during different monsoon seasons. Austr. J. Freshwater Res. 43, 1517–1533.
Umitsu, M., 1985. Natural levees and landform evolution in the Bengal lowland. Geogr. Rev. Jpn. 58, 149–164.
Umitsu, M., 1987. Late Quaternary sedimentary environment and landform evolution in the Bengal lowland. Geogr. Rev. Jpn. 60, 164–178.
Umitsu, M., 1993. Late Quaternary sedimentary environments and landforms in the Ganges delta. Sediment. Geol. 83, 177–186.
Wright, L.D., Coleman, J.M., 1973. Variations in morphology of major deltas as functions of ocean wave and river discharge regimes. Bull. AAPG 57, 370–398.
Wright, L.D., Coleman, J.M., 1974. Mississippi River mouth processes: Effluent dynamics and morphologic development. J. Geol. 82, 751–778.
Wright, L.D., Nittrouer, C.A., 1995. Dispersal of river sediments in coastal seas: Six contrasting cases. Estuaries 18, 494–508.
Wyrtki, K., 1973. Physical oceanography of the Indian Ocean. In: Zeitzschel, B. (Ed.), Ecology Studies, The Biology of the Indian Ocean. Springer, New York, pp. 18–36.
Xiqing, C., 1996. An integrated study of sediment discharge from the Changjiang River, China, and the delta development since the mid-Holocene. J. Coastal Res. 12, 26–37.